

Rotordynamic Behavior Analysis of a Short Labyrinth Gas Seal Using CFD Tool

Mohamed KAMOUNI

Sidi Mohamed ben Abdelleh University, Fez, Morocco

Abstract—Labyrinth seals are mechanical element commonly used to reduce leakage in interfaces between rotating and stationary parts of turbomachines. However, these elements may modify the shaft line dynamics. Thus, accurate predictions and efficient controls of leakage and seal influence on the rotordynamic stability area very important task to improve efficiency and performance of rotating machines using this kind of seals. The main purpose of this paper is to build a full 3D eccentric CFD model providing accurate leakage and rotordynamic coefficients for a short straight labyrinth seal. The seal has four teeth fixed on the rotor and the work fluid is air. The model accuracy has been validated on experimental measurements of the pressure distribution along and around the seal. Moreover, a parametric study has been conducted to show the effects of pressure ratio along with three mean radial clearances on leakage flow and rotor dynamic characteristics of the seal and obtained results are presented.

Index Terms—Labyrinth seal, Leakage, Rotor dynamic coefficients, CFD, Swirl, Whirl, Clearance.

1 INTRODUCTION

ANNULAR gas seals are key element to dissipate energy and minimize leakage flow rate between a rotating shaft and a stationary housing. Along with leakage performance, the importance of rotordynamic assessment for noncontact annular gas seals is well recognized. As the most common type of annular gas seals, labyrinth seals are widely used in compressors and turbines. Figure 1 shows three compressor labyrinth sites denoted 1, 2 and 3 corresponding to shaft seal, eye seal and balance drum seal, respectively.

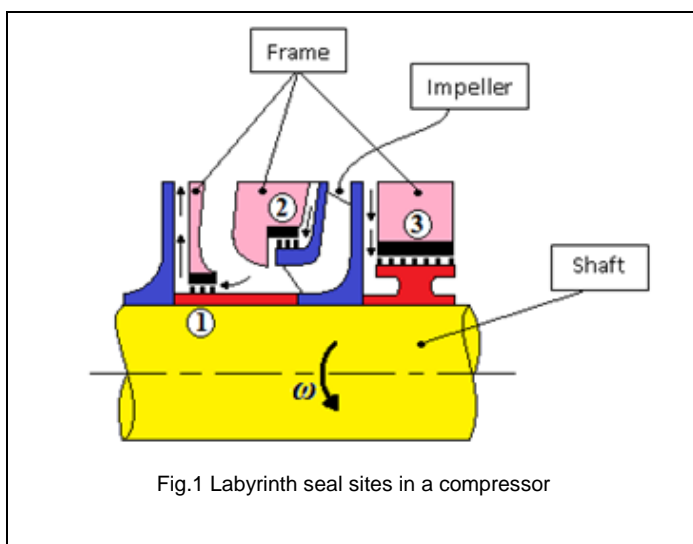


Fig.1 Labyrinth seal sites in a compressor

To meet the sealing requirements, there are many types of labyrinth seal to allow adequate choice for a sealing solution: straight, stepped, staggered, inclined, etc. [1]. The leakage flow rates and rotordynamic coefficients of labyrinth gas seals are functions of the fluid properties, operational conditions, and geometrical parameters [2,3]. All these parameters act simultaneously and may change. It results that static and

dynamic behavior prediction remains a demanding and challenging task [4] for labyrinth gas seals. The complex working flow passing through these seals has been the subject of many worldwide experimental and theoretical studies in the last three decades.

In the experimental field, Meyer and Lowrie [5] and Mehta and Childs [6] experimentally studied the leakage characteristics of straight-tooth and slanted-tooth labyrinth seals. Results show that the slanted-tooth labyrinth seal leaks approximately 10% less than the straight-tooth labyrinth seal. Gamal and Vance [7] experimentally studied the influences of tooth number, tooth thickness, and eccentricity on the leakage flow rates through labyrinth seals. Results show that doubling tooth thickness reduces the leakage by up to 20%, and a flat-tipped tooth is more effective in limiting leakage than a bevel-tipped tooth. Childs and Scharrer [8] and Vance et al. [9] performed extensive experiments to measure the rotordynamic coefficients of both tooth-on-stator and tooth-on-rotor labyrinth seals. Experimental results show that tooth-on-rotor labyrinth seals possess smaller damping and are modestly less stable than tooth-on-stator labyrinth seals. Picardo and Childs [10] presented measurement results of rotordynamic coefficients for a tooth-on-stator labyrinth seal with two clearances of 0.1 and 0.2 mm. The results show that the effective damping of the labyrinth seal is almost completely lacking of sensitivity to changes in sealing clearance. Childs et al. [11] experimentally investigated the effect of different swirl brakes (no swirl brake, straight swirl brake, and negative-swirl brake) on the rotordynamic characteristics of the labyrinth seal. The results show that the negative-swirl brake has the most remarkable effect. It causes change in the sign of cross-coupled stiffness to become stabilizing and gives rise to a marked increase in effective damping.

In the theoretical field, rotordynamic modelling of labyrinth seals was mainly based on the bulk-flow approach. Iwatsubo was the first to develop this approach in 1980 [12]. The

primary advantage of bulk-flow models is that they can predict the seal rotor dynamic coefficients with efficient computational time. However, these models lack flow details and rely on correlations and empirical corrections such as flow coefficients and friction factors [13, 14] that may change for varying operational condition and seal geometry. Due to the limitations of this approach, the computational fluid dynamics (CFD) methods for solving Navier- Stokes equations were applied to obtain more satisfactory predictions for various seal types at different boundary and operating conditions. With the increased availability of computational resources, comprehensive CFD models are now gradually replacing the bulk-flow approach in the seal performance analysis. Currently, several recent works applied commercial CFD codes to metproblems of labyrinth gas seal rotordynamics [15, 16]. The accuracy of predictions compared to measurements was not always sufficient. One can conclude that CFD technique is a powerful tool, but further research is still needed to make CFD calculations a standard part of the design process for the prediction of rotordynamic coefficients of labyrinth gas seals.

It follows that, additional investigations are needed to accurately model and simulate turbulent flows through labyrinth seals in order to more understand their static and dynamic behaviour. In this contest, the present work attempts to calculate the leakage flow and rotor dynamic coefficients for a short eccentric labyrinth gas seal based on tridimensional CFD techniques solving the general Reynolds Averaged Navier-Stokes equations along with appropriate turbulence model. This work focuses on the effect of pressure ratio and mean radial clearance on the static and dynamic characteristics for this kind of seals.

2 GEOMETRY AND CFD MODEL OF THE SEAL

2.1 Seal Geometry

The straight labyrinth seal object of this study has four teeth fixed on the rotor lateral surface. The 2-D seal geometry is shown in figure 1 and the seal dimensions are summarized in table 1.

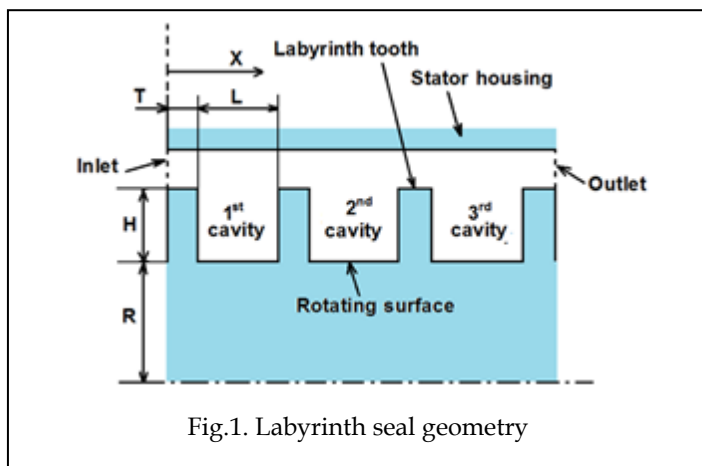


Fig.1. Labyrinth seal geometry

The seal working fluid is air. A cut section of the 3-D fluid computational domain is shown in figure 2. The teeth are

represented by circumferential grooves in this computational

TABLE 1
GEOMETRICAL DIMENSIONS OF THE SEAL

| | |
|-------------------------|------------------------|
| Rotor radius, R | 93.66 mm |
| Tooth width, L | 12.7 mm |
| Tooth thickness, T | 3.18 mm |
| Tooth height, H | 7.94 mm |
| Mean clearance width, C | 0.25, 0.5 and 0.949 mm |

domain.

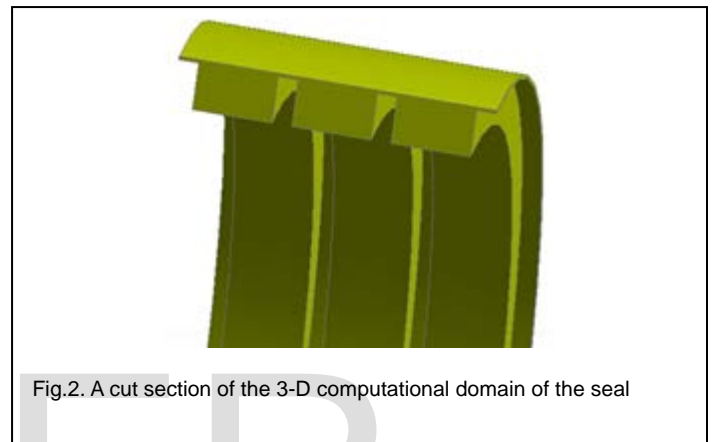


Fig.2. A cut section of the 3-D computational domain of the seal

2.2 Governing Equations

The turbulent flow through the seal is governed by the continuity and momentum equations.

Continuity equation:

$$\frac{\partial \rho}{\partial t} + \frac{\partial(\rho u_i)}{\partial x_i} = 0 \quad (1)$$

Momentum equation:

$$\frac{\partial \rho u_i}{\partial t} + \frac{\partial(\rho u_i u_j)}{\partial x_j} = -\frac{\partial P}{\partial x_i} + \frac{\partial}{\partial x_j} \left[\mu_{eff} \left(\frac{\partial u_i}{\partial x_j} + \frac{\partial u_j}{\partial x_i} \right) \right] + S_M \quad (2)$$

where

S_M is the sum of body forces

μ_{eff} is the effective viscosity accounting for turbulence.

$$\mu_{eff} = \mu + \mu_t \quad (3)$$

μ_t is the turbulence viscosity and μ is a constant.

These equations are completed by the (k, ω) SST turbulence model.

2.3 Meshing

For the given seal geometry, an appropriate mesh is required to describe correctly the flow within the seal. Hexahedral mesh elements were used to create three dimensional non-uniform structured meshes in the entire computational domain. An adequate mesh refinement is allowed to the clearance area and boundary layers to accurately calculate desired physical parameters of the flow

within the seal. Fig. 5 shows a cut section of generated computational grids in the 3-D computational domain.

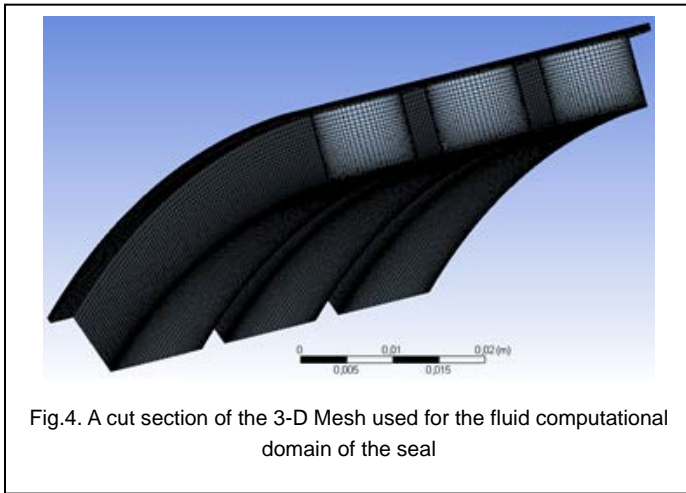


Fig.4. A cut section of the 3-D Mesh used for the fluid computational domain of the seal

2.4 Rotating Frame

Observing the motion of rotor-seal system from a stationary frame, the rotor is spinning at the speed ω while also whirling at the speed Ω at the same time, which means that the location of rotor and thus the shape of mesh are changing all the time. So it is actually a transient problem involved with mesh moving. To avoid a transient analysis and moving mesh, a rotating frame with the speed Ω was applied as shown in figure 5. In the rotating frame, the rotor itself spins at the speed $(\omega - \Omega)$, while the stator spins at the speed Ω in the opposite direction to the frame. Thus it becomes a steady state problem and there is no mesh moving.

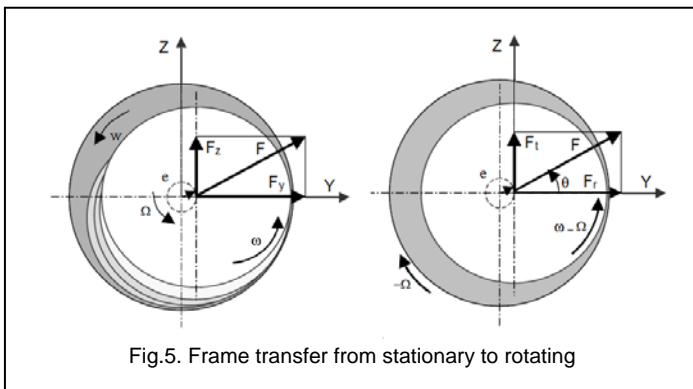


Fig.5. Frame transfer from stationary to rotating

2.5 Rotordynamic Coefficients

The fluid driving forces exerted on the rotor can be obtained at each whirl frequency Ω by integration of the static pressure along and around the seal rotor surface.

$$F_y = R \iint p \cos\theta \, d\theta \, dx \quad (4)$$

$$F_z = R \iint p \sin\theta \, d\theta \, dx \quad (5)$$

As shown in figure 6, a positive radial force is a centering force while a negative radial force is a decentering one. A

positive tangential force is a forward whirl force while a negative tangential force is a backward whirl force.

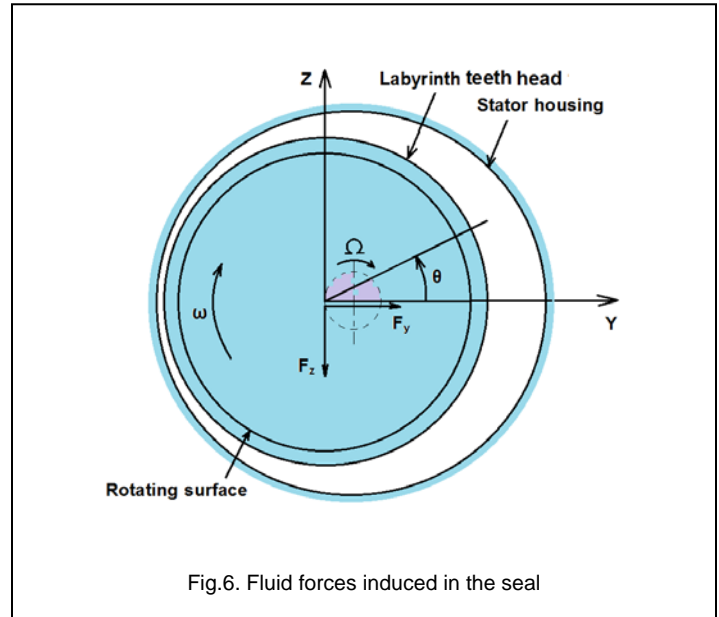


Fig.6. Fluid forces induced in the seal

For small motion of the rotor center about a centered position, the relation between the reaction-force components and the shaft motion is defined by the following linearized dynamic model.

$$\begin{Bmatrix} F_y \\ F_z \end{Bmatrix} = \begin{bmatrix} K & k \\ -k & K \end{bmatrix} \begin{Bmatrix} y \\ z \end{Bmatrix} + \begin{bmatrix} D & d \\ -d & D \end{bmatrix} \begin{Bmatrix} \dot{y} \\ \dot{z} \end{Bmatrix} \quad (6)$$

where (y, z) define the lateral motion of the rotor center relative to the stator, (F_y, F_z) are the components of the reaction force acting on the rotor. (K, k) and (D, d) represent the direct and cross-coupled stiffness and damping coefficients, respectively. The cross-coupled terms (k, d) arise from the fluid's circumferential velocity component. If the shaft center moves in a circular orbit with rayon e , then the rotation displacement vector to the shaft center has coordinates:

$$y = e \cos(\Omega t) \quad (7)$$

$$z = e \sin(\Omega t) \quad (8)$$

The radial force component F_r and the tangential force component F_t can be formulated as follows:

$$\frac{F_r(\Omega)}{e} = \frac{F_y(t=0)}{e} = -d\Omega - K \quad (9)$$

$$\frac{F_t(\Omega)}{e} = \frac{F_z(t=0)}{e} = k - D\Omega \quad (10)$$

The direct stiffness coefficient K and the cross-coupled damping coefficient d can be obtained employing a linear

regression of the calculated radial force for two values of Ω (e.g. $\Omega = 0$ and $\Omega = 0.5\omega$) in equation (9). The direct damping coefficient D and the cross-coupled stiffness coefficient k can be determined from linear regression of the calculated tangential force for two values of Ω (e.g. $\Omega = 0$ and $\Omega = 0.5\omega$) in equation (10).

3 RESULTS AND DISCUSSIONS

3.1 Validation of the CFD Model

The developed model has been solved in the given seal respecting the boundary conditions used by Rajakumar and Sisto [17] and summarized in table 2. The negative signs of the rotating speed and the inlet swirl velocity indicate that the rotor turns in the clockwise direction as per the angle sign convention shown in figure 6.

The static pressure distribution along and around the seal has been locally calculated in each mid-cavity of the seal.

TABLE 2
OPERATING CONDITIONS OF THE SEAL

| | |
|--------------------------------|------------|
| Eccentricity ratio, ϵ | 43 % |
| Rotating speed, ω | -2025 rpm |
| Inlet pressure, P_{in} | 1.1077 MPa |
| Outlet pressure, P_{out} | 1.033 MPa |
| Inlet swirl velocity, W_{in} | -49.8 m/s |

Figures 7 and 8 show a comparison between the current CFD predictions and the available results of experiments made on the same seal by Rajakumar and Sisto [17]. It can be easily seen that predictions are in good agreement with measurements. Additionally, figure 7 shows that the pressure drops from the inlet pressure at left to the outlet pressure at right, and the pressure is almost equal in the same cavity interior.

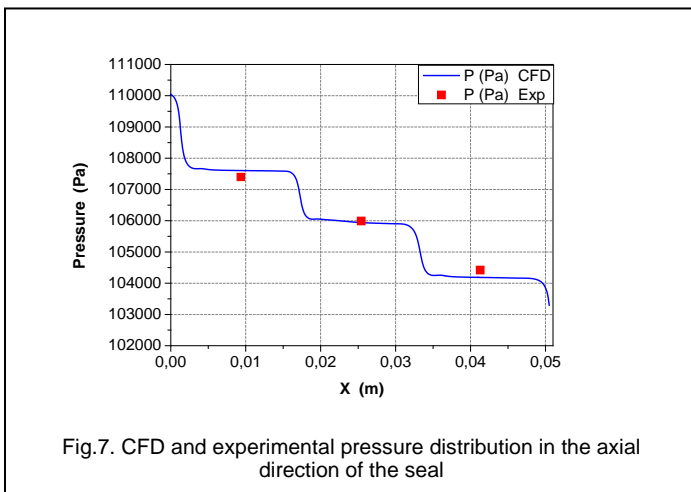


Fig.7. CFD and experimental pressure distribution in the axial direction of the seal

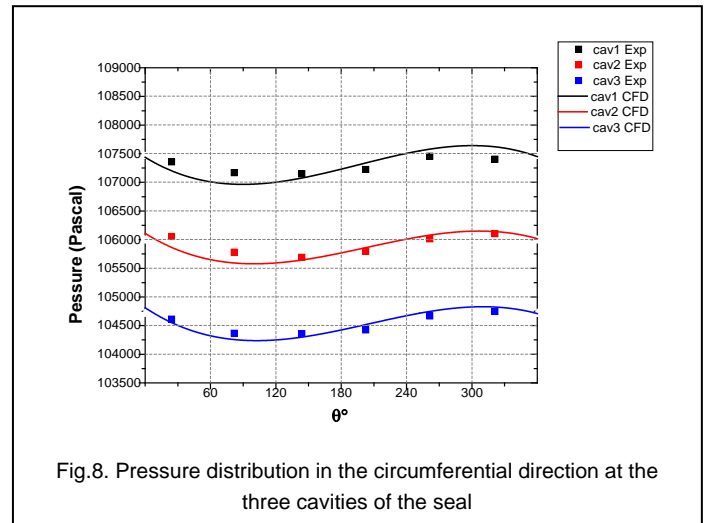


Fig.8. Pressure distribution in the circumferential direction at the three cavities of the seal

Figure 9 shows contours of the static pressure in an axial radial plane of the seal. The static pressure drop starts from the seal inlet pressure to reach the outlet pressure at the seal exit. The quasi same color in each cavity interior confirms that pressure is quasi constant in each cavity interior. Furthermore, it is shown that pressure drop mainly occurs in the left zone of each cavity at the labyrinth tooth throttling.

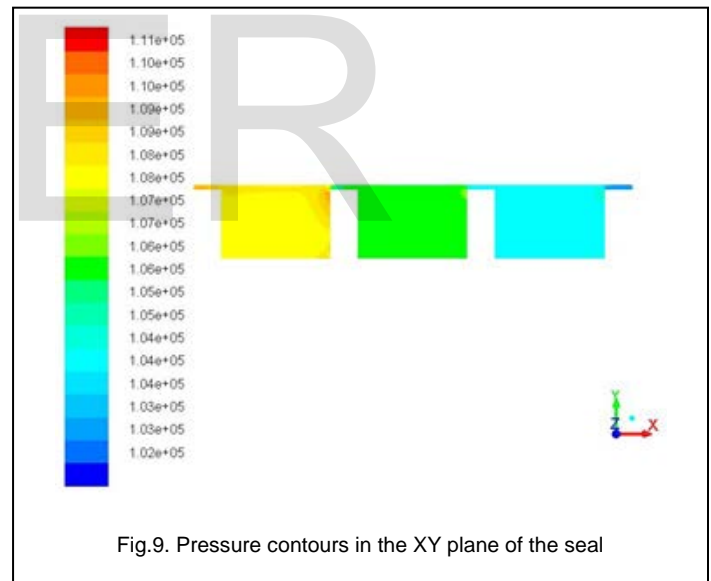


Fig.9. Pressure contours in the XY plane of the seal

3.2 Effects of Pressure and Clearance on Leakage

The operating conditions used in this section are summarized in table 3.

TABLE 3
OPERATING CONDITIONS OF THE SEAL

| | |
|--|----------------------|
| Eccentricity ratio, ϵ | 10 % |
| Rotating speed, ω | -2025 rpm |
| Inlet pressure ratio, P_{in}/P_{out} | 1.072, 2, 4, 6 and 8 |
| Inlet swirl, $W_{in} = 0.5R\omega$ | -9.93 m/s |

Figure 10 represents leakage flow versus the pressure ratio (P_{in}/P_{out}) with the mean radial clearance as a parameter. This figure shows that the leakage increases with increasing pressure ratio and mean radial clearance. Furthermore, it can be stated that roughly for this prediction range, the leakage flow increases nearly in the same proportion with increasing mean radial clearance. In addition, the leakage flow becomes more sensitive to pressure ratio variations with high radial clearances.

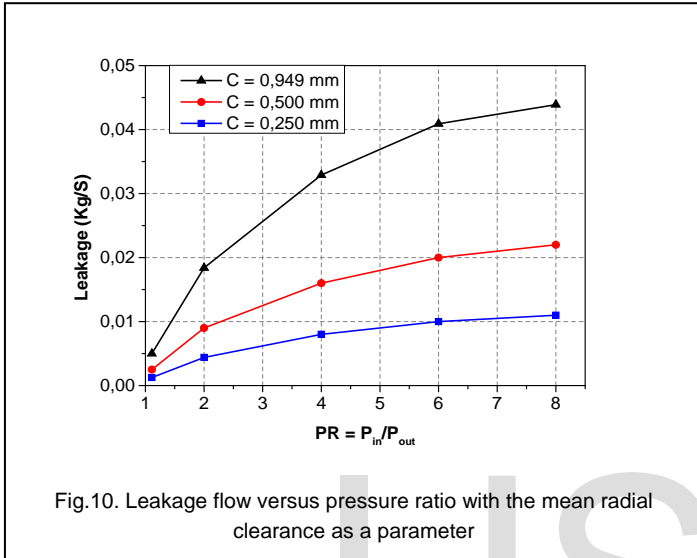


Fig.10. Leakage flow versus pressure ratio with the mean radial clearance as a parameter

3.3 Effects of Pressure and Clearance on Rotor-dynamic Coefficients

This section deals with the dynamic behavior of the seal based on the operating conditions given in table 3. Figures 11 and 12 represent respectively direct and cross coupled stiffness coefficients versus the pressure ratio (P_{in}/P_{out}) with the mean radial clearance as a parameter. Figure 11 shows that direct stiffness is always negative and its magnitude increases with increasing pressure ratio and radial clearance. Additionally, it can be easily seen that direct stiffness coefficient magnitude is more sensitive to changes in pressure ratio with high radial clearances. An opposite effect is observed in Figure 12 for the cross-coupled stiffness which is significantly higher and more sensitive to change in pressure ratio with small radial clearances. In other words, since the cross-coupled stiffness is a destabilizing influence, the rotor system becomes more unstable for small clearance cases. It can be stated that more the pressure ratio is low and the mean radial clearance is high, more the seal is dynamically stable.

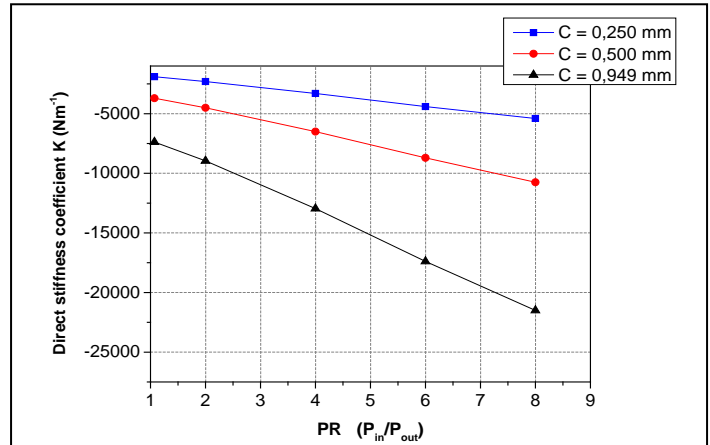


Fig.11. Direct stiffness coefficient versus pressure ratio with the inlet swirls ratio as a parameter

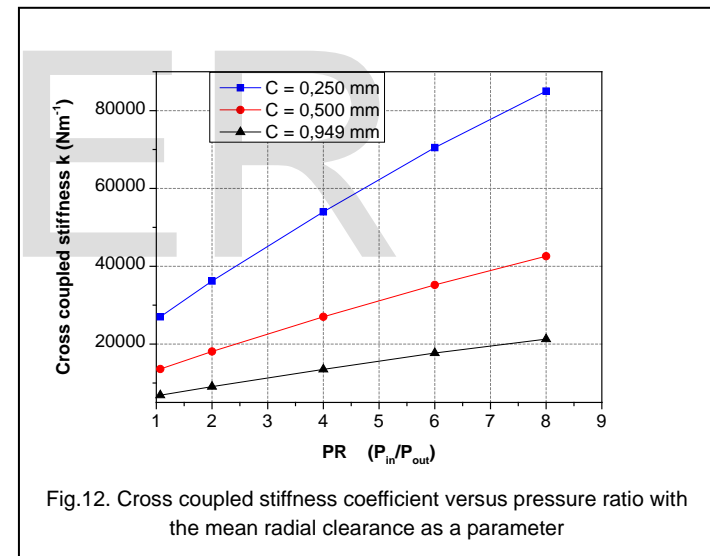
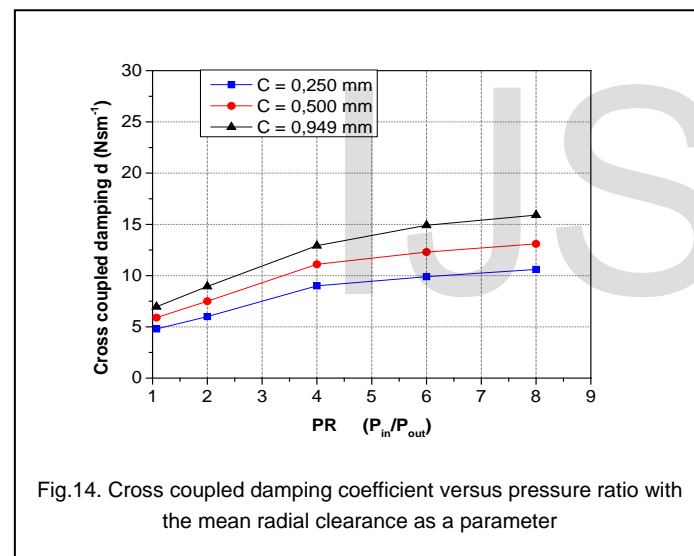
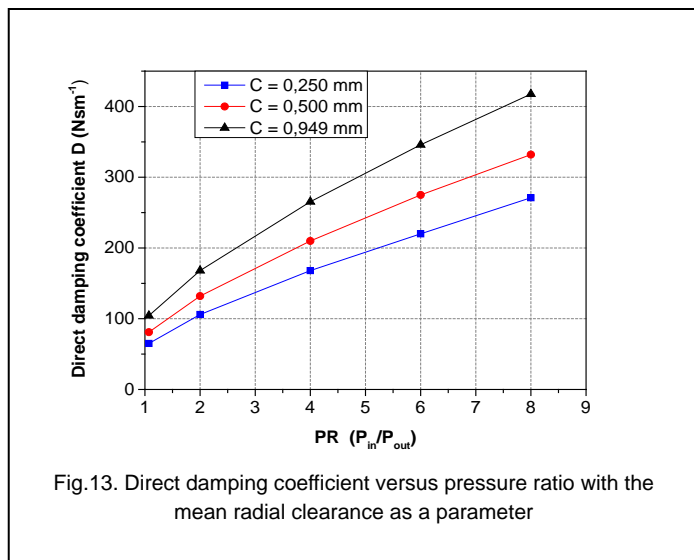


Fig.12. Cross coupled stiffness coefficient versus pressure ratio with the mean radial clearance as a parameter

Figures 13, and 14 represent respectively direct and cross coupled damping coefficients versus the pressure ratio (P_{in}/P_{out}) with the mean radial clearance as a parameter. Both these coefficients increase slightly with increasing pressure ratio and mean radial clearance. According to the current predictions range, while direct damping increasing is nearly linearly with pressure ratio and radial clearance, the cross-coupled damping increasing remains less important. In one hand, the direct damping coefficient is known to have a stabilizing influence; hence maximum values are beneficial for this coefficient. In the other hand, cross coupled damping coefficients is known to be with small magnitudes as it is the case here and without any recognized influence from a dynamic stability point of view.

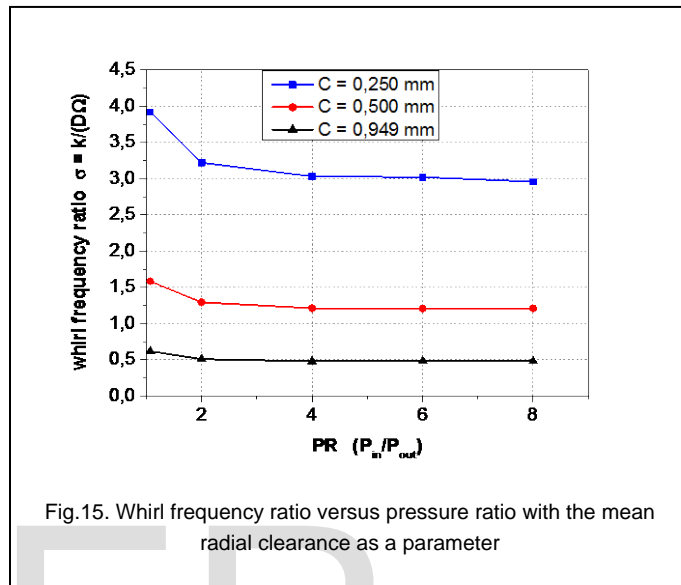


To compare the destabilizing influence of cross-couples stiffness to the stabilizing influence of direct damping, the whirl frequency ratio σ is introduced as follows:

$$\sigma = \frac{k}{D\Omega} \quad (11)$$

This ratio provides an assessment for the dynamic stability of the seal. More the whirl frequency ratio is smaller more the seal is dynamically stable. Figure 14 represents the whirl frequency ratio versus the pressure ratio with the mean radial clearance as a parameter. This figure shows that grossly in this predictions range, this parameter is very slightly influenced with increasing pressure ratio. However, it is easily seen that the whirl frequency ratio is more influenced by the radial

clearance variations. It results that although small radial clearances are important in reducing losses in terms of leak rate, they should be well controlled in terms of dynamic stability of the seal. Thus, according to the leakage and whirl frequency ratio results in the given predictions range, a reasonable mean radial clearance as 0.25 mm associated with the pressure ratio ($P_{in}/P_{out} = 8$) could be considered the optimal solution for this studied labyrinth seal.



4 CONCLUSION

A tridimensional model to analyze turbulent gas flow through short straight labyrinth seal has been developed based on CFD calculation. With full respect for the given operating conditions of the seal, this model solves the general Reynolds Averaged Navier-Stokes equations along with the $k-\omega$ SST turbulence model. Predictions accuracy has been validated on measurements of the pressure distribution along and around the seal. The pressure is almost quasi equal in each cavity interior and pressure drop mainly occurs in the left zone of each cavity at the labyrinth tooth throttling. Leakage and rotordynamic coefficient of the seal have been calculated respecting prior operating conditions. The leakage flow increases nearly in the same proportion with increasing mean radial clearance and becomes more sensitive to pressure ratio variations with high radial clearances. The whirl frequency ratio has been introduced to compare the destabilizing influence of cross-couples stiffness to the stabilizing influence of direct damping. Although small radial clearances are important in reducing losses in terms of leak rate, they should be well controlled in terms of dynamic stability of the seal. According to the given predictions range, a mean radial clearance of 0.25 mm associated with the pressure ratio ($P_{in}/P_{out} = 8$) is an optimal solution for this studied labyrinth seal.

References

[1] R. E., Chupp, R. C., Hendricks, S. B., Lattime, and B. M., Steinetz, "Sealing in Turbomachinery," NASA Glenn Research Center,

- Cleveland, OH, NASAPaper No. TM 214341, 2006.
- [2] Li, J., Choudhury, P. D., and Kushner, F., "Evaluation of Centrifugal Compressor Stability Margin and Investigation of Antiswirl Mechanism," Proceedings of the 32nd Turbomachinery Symposium, Turbomachinery Lab., Texas A&M Univ., College Station, TX, Sept. 2003, pp. 49-57.
- [3] D.W., Childs, and J. M., Vance, "Annular Seals and the Rotordynamics of Compressors and Turbines," Proceedings of the 26th Turbomachinery Symposium, Turbomachinery Lab., Texas A&M Univ., College Station, TX, Sept. 1997, pp. 201-220.
- [4] M., Wensheng, C., Zhaobo, and J., "Yinghou, Leakage and Whirl Speed Study in Labyrinth Seal Using CFD," International Conference on Electronic & Mechanical Engineering and Information Technology (EMEIT), Harbin, China, Aug. 12-14, 2011, pp. 592-595.
- [5] C., Meyer, , and J. A., Lowrie, "The Leakage Through Straight and Slant Labyrinths and Honeycomb Seals," ASME Journal of Engineering for Gas Turbines and Power, Vol. 97, No. 4, 1975, pp. 495-501.
- [6] N. J., Mehta, and D.W., Childs, "Measured Comparison of Leakage and Rotordynamic Characteristics for a Slanted-Tooth and a Straight-Tooth Labyrinth Seal," ASME Journal of Engineering for Gas Turbines and Power, Vol. 136, No. 1, 2014, Paper 012501.
- [7] A. M., Gamal, and , J. M., Vance "Labyrinth Seal Leakage Tests: Tooth Profile, Tooth Thickness, and Eccentricity Effects," ASME Journal of Engineering for Gas Turbines and Power, Vol. 130, No. 1, 2008, Paper 012510.
- [8] D. W., Childs, and J., Scharrer, "Experimental Rotordynamic Coefficient Results for Teeth-on-Rotor and Teeth-on-Stator Labyrinth Gas Seals," ASME Journal of Engineering for Gas Turbines and Power, Vol. 108, No. 4, 1986, pp. 599-604.
- [9] J. M., Vance, J. J., Zierer, and E. M., Conway, "Effect of Straight Through Labyrinth Seals on Rotordynamics," Proceedings of the ASME Vibration and Noise Conference, American Soc. of Mechanical Engineers, Two Park Avenue, NY, Sept. 1993, pp. 159-171.
- [10] A., Picardo, and D.W., Childs, "Rotordynamic Coefficients for a Tooth-on-Stator Labyrinth Seal at 70 Bar Supply Pressures: Measurements Versus Theory and Comparisons to a Hole-Pattern Stator Seal," ASME Journal of Engineering for Gas Turbines and Power, Vol. 127, No. 4, 2005, pp. 843-855.
- [11] Childs, D. W., Mclean, J. E., Zhang, M., and Arthur, S. P., "Rotordynamic Performance of a Negative-Swirl Brake for a Tooth-on-Stator Labyrinth Seal," American Soc. of Mechanical Engineers Paper GT2014-25577, 2014.
- [12] T. Iwatsubo, "Evaluation of Instability Forces of Labyrinth Seals in Turbines or Compressors," In Proc. Rotordynamic Instability Problems in High Performance Turbomachinery, " NASA CP-2133, Texas A&M University, pp 139-167, 1980.
- [13] G. G. Hirs, "A Bulk Flow Theory for Turbulent in Lubricant Films", Journal of Lubrication Technology, pp.137-146, 1973.
- [14] L. Moody, "Friction Factors for Pipe Flow," Transactions of the ASME, Vol. 66, pp. 671, 1944.
- [15] A. Pugachev., U. Kleinhansand and M. Gaszner. " Prediction of Rotordynamic Coefficients for Short Labyrinth Gas Seals Using Computational Fluid Dynamics", ASME, Journal of Engineering for Gas Turbines and Power, 062501, Vol. 134, pp. 1-10, 2012.
- [16] D. Sun, S. Wang, C. Fei, Y. Ai and K. Wang "Numerical and Experimental Investigation on the Effect of Swirl Brakes on the Labyrinth Seals," ASME, Journal of Engineering for Gas Turbines and Power, 032507, V 138, pp. 1-12, 2016.
- [17] C. Rajakumar and F. Sisto, "Experimental Investigations of Rotor Whirl Excitation Forces Induced by Labyrinth Seal Flow," ASME Journal of Vibration and Acoustics, vol. 112, pp. 515-522, 1990.